Observation of a narrow structure in $^1H(\gamma,K^0_S)X$ via interference with ϕ-meson production

M. J. Amaryan,[1,*] G. Gavalian,[1] C. Nepali,[1] M. V. Polyakov,[2,3] Ya. Azimov,[3] W. J. Briscoe,[4] G. E. Dodge,[1] C. E. Hyde,[1] F. Klein,[5] V. Kuznetsov,[6,7] I. Strakovsky,[4] and J. Zhang[8]

[1]*Old Dominion University, Norfolk, Virginia 23529, USA*
[2]*Institut für Theoretische Physik II, Ruhr–Universität Bochum, D-44780 Bochum, Germany*
[3]*Petersburg Nuclear Physics Institute, Gatchina, St. Petersburg 188300, Russia*
[4]*The George Washington University, Washington, DC 20052, USA*
[5]*Catholic University of America, Washington, DC 20064, USA*
[6]*Kyungpook National University, 702-701, Daegu, Republic of Korea*
[7]*Institute for Nuclear Research, 117312, Moscow, Russia*
[8]*Thomas Jefferson National Accelerator Facility, Newport News, Virginia 23606, USA*

(Received 20 October 2011; revised manuscript received 29 February 2012; published 26 March 2012; publisher error corrected 29 March 2012)

We report observation of a narrow peak structure at ∼1.54 GeV with a Gaussian width $\sigma = 6$ MeV in the missing mass of K_S in the reaction $\gamma + p \to pK_SK_L$. The observed structure may be due to the interference between a strange (or antistrange) baryon resonance in the pK_L system and the $\phi(K_SK_L)$ photoproduction leading to the same final state. The statistical significance of the observed excess of events estimated as the log-likelihood ratio of the resonant signal + background hypothesis and the ϕ-production-based background-only hypothesis corresponds to 5.3σ.

DOI: 10.1103/PhysRevC.85.035209 PACS number(s): 13.60.Rj, 14.40.−n, 12.38.−t, 25.20.Lj

I. INTRODUCTION

The nonrelativistic constituent quark model (NRCQM) describes mesons and baryons as $q\bar{q}$ pairs and $3q$ configurations, respectively. Proposed originally to describe classification of light mesons and baryons consisting of u, d, and s quarks, NRCQM appears to be very successful. In particular, in the baryon sector, which is more relevant to this study, it unifies all known light baryons in terms of two irreducible representations of SU(3) symmetry: 1. spin 1/2 baryons belonging to the octet (**8**) and 2. spin 3/2 baryons belonging to the decuplet (**10**). Furthermore, states with different isospin projections, but the same hypercharge, form isospin multiplets.

However, the NRCQM is a phenomenological model. It is not derived from first principles of quantum chromodynamics (QCD), the fundamental theory of strong interactions, and therefore the existence of other states beyond its limits cannot be excluded. Among such states are hybrids, glueballs, and multiquark states. The observation of these new QCD configurations, or understanding the reason why they are not realized in nature, will help us to obtain an important insight into the underlying dynamics of strong interactions and properties of QCD in the nonperturbative regime.

Discussions of multiquark states go back to the early days of the quark model and unsuccessful experimental efforts to observe such configurations span decades. However, recently there appeared a striking prediction of the chiral quark soliton model [1] for an entire new family of five-quark (pentaquark) states that belong to the $\bar{\mathbf{10}}$ (antidecuplet) representation of SU(3) symmetry, creating a new wave of excitement in the field of hadronic physics. In particular, an explicitly exotic pentaquark state, with minimal quark content $uudd\bar{s}$, lying on the apex of the new representation of SU(3) symmetry and called now Θ^+, was predicted to have mass $M_{\Theta^+} = 1.53$ GeV and narrow width $\Gamma < 15$ MeV. From an experimental point of view this excitement was due to the narrow width of the predicted pentaquark state, which would make its observation much easier, due to its simple decay mode to K^+n or K^0p, and finally due to its relatively low mass, which makes its production possible at many experimental facilities.

Inspired by this prediction, the first experimental results of the observation of Θ^+ were obtained and reported by the SPring-8 Collaboration in a low-energy photoproduction experiment [2] and independently by the DIANA Collaboration [3] in a formation reaction with a low-energy kaon beam. Subsequently, positive claims followed by the CLAS [4,5], SAPHIR [6], HERMES [7], ZEUS [8], and SVD [9] Collaborations. In parallel, negative results were reported by several groups: HERA-B [10], HyperCP [11], BES [12], ALEPH [13], and BABAR [14].

The common feature of most experimental results was that they were reported out of nondedicated experiments. It was not until 2004 that the CLAS Collaboration performed dedicated high-statistics photoproduction experiments both on deuterium and hydrogen targets. It was found, first of all, that the previous measurement on the deuterium target by CLAS [4] was not reproduced in the new measurement, despite order of magnitude higher statistics [15]. It is now understood [15] that the level of background in the first paper was underestimated and therefore the observed signal was statistically not so significant. The search for Θ^+ in the high-statistics CLAS measurement of the reaction $\gamma + p \to \bar{K}^0K^+n$ in CLAS [16] was negative. This is the same channel in which the SAPHIR Collaboration reported a positive result [6]. It is worthwhile to

*Corresponding author: mamaryan@odu.edu

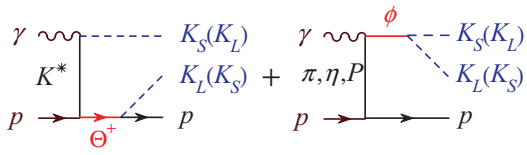

FIG. 1. (Color online) Two different subprocesses in the reaction $\gamma p \to pK_SK_L$ that can lead to the same final state: $\Theta^+(pK^0)$ production (left) and ϕ-meson production (right).

mention that there is a significant difference in the geometric acceptance of CLAS and SAPHIR in the forward direction: on the order of a few percent for the $\pi^+\pi^-K^+$ triple coincidence in CLAS and almost full coverage in the forward angles for SAPHIR. This will affect the sensitivity if the Θ^+ production is strongly forward peaked. In addition, the search for the Θ^+ was performed for the first time in the reaction $\gamma + p \to \bar{K}^0K^0p$, which also did not result in a Θ^+ signal [16]. Before publication of the high-statistics CLAS data, the experimental situation was considered to be uncertain. The high-statistics CLAS publications [15,16] lowered the confidence for the existence of the Θ^+ pentaquark [17], although the papers themselves quote only upper limits on the Θ^+ photoproduction cross section, estimated to be on the order of a few nanobarns. Detailed reviews of the experimental situation can be found in [18,19]. Critical comparison of positive and negative results was presented in [20]. Meanwhile, the SPring-8 Collaboration published a new paper [21], where they reproduced their previous result with increased statistics on a deuteron target, and the DIANA Collaboration confirmed their previous result with increased statistics in renewed analyses [22,23].

The analysis reported here was performed in an attempt to increase the experimental sensitivity of the CLAS setup to a small Θ^+ signal. One possible way to do so is to exploit quantum mechanical interference to enhance the small amplitude of the Θ^+ by some other resonance with a strong production cross section leading to the same final state. Numerous examples of how interference helps to enhance the faint signal of one resonance by a stronger signal of another resonance are presented in a recent review by Azimov [24]. Such a possibility for the search of Θ^+ can be realized in the reaction $\gamma p \to pK_SK_L$, where, as was proposed in [25], one can use photoproduction of the $\phi(K_SK_L)$ meson to enhance a baryon resonance in either the pK_S or pK_L system. The two processes leading to the same pK_SK_L final state are shown in Fig. 1. Since both $\gamma p \to p\phi \to pK_SK_L$ and $\gamma p \to \Theta^+\bar{K}^0 \to pK_SK_L$ reactions have the same final state, quantum mechanically they must interfere. As a result of the interference, the small amplitude of a possible Θ^+ (or any other baryon with a similar decay mode) production would be multiplied by the large ϕ production amplitude, thus increasing sensitivity to a possible signal of the strange (or antistrange) baryon.

II. EXPERIMENT

The present study is based on the same data set collected in 2004 (g11a run period) using the CLAS detector at the Thomas Jefferson National Accelerator Facility (TJNAF) and analyzed previously [16]. The experiment was performed using a photon beam produced through bremsstrahlung from a 4.02-GeV initial electron beam from the Continuous Electron Beam Accelerator Facility (CEBAF) at Jefferson Lab.

A scintillator hodoscope system, combined with a dipole magnet, was used to tag the photon energy in the range of 0.8 to 3.8 GeV, with a resolution of 0.1% of the incident electron energy. A different set of scintillators is used for the timing measurement. Surrounding the target segmented (for each sector) scintillator counters were placed for triggering the event. The CLAS detector is described in detail elsewhere [26].

In this experiment the photon beam was incident on a 40-cm-long liquid hydrogen target, centered 10 cm upstream from the center of the CLAS detector. Particles from the reaction were detected in the CLAS detector, consisting of six equal sectors, equipped with time-of-flight scintillator counters, electromagnetic calorimeters, drift chambers, and Čerenkov counters, covering nearly 4π solid angle. The drift chambers consisted of three layers, each layer having two sublayers. The second layer was placed inside of a toroidal magnetic field, used to bend the trajectories of the charged particles in order to measure their momenta. The momentum resolution of the CLAS detector is momentum dependent and on average is on the order of $\Delta P/P \sim 0.5\%$. The charged particle identification is based on simultaneous measurement of their momenta and the time of flight. The CLAS standard particle identification scheme is used to select charged particles in the final state. The photon beam energy correction and charged particle momentum correction are based on the code developed by the g11 run group and used in the previous analysis [16]. The raw data used in this analysis were processed in the same way as in [16], including corrections for the energy loss of charged particles in the target, uncertainties in the magnetic field, and misalignments of drift chambers.

III. ANALYSIS

A. Event selection and reconstruction of the final state

Events for this analysis are selected requiring at least three charged tracks in the final state identified as a proton, π^+, and π^-. The initial photon is chosen to be within 1 ns of the start time defined by the start counter, and it was required to have only one hit in the tagger within 1.5 ns of the start time. K_S is reconstructed in the invariant mass of two pions and K_L in the missing mass of detected particles, $M(K_L)^2 = M_X(pK_S)^2 = (P_\gamma + P_t - P_{K_S} - P_p)^2$, where P_i are four-momenta of the photon, target proton, K_S, and final-state proton. The search for a resonance in the KN system can be done either in the invariant mass of the proton and K_S or in the missing mass of K_S. To identify the reconstructed K_S and the final KN state with good mass resolution and acceptable signal-to-background ratio the following cuts were implemented (hereinafter referred to as vertex cuts):

(i) The proton track must come within 2 cm of the photon beam line; the midpoint of the shortest line between

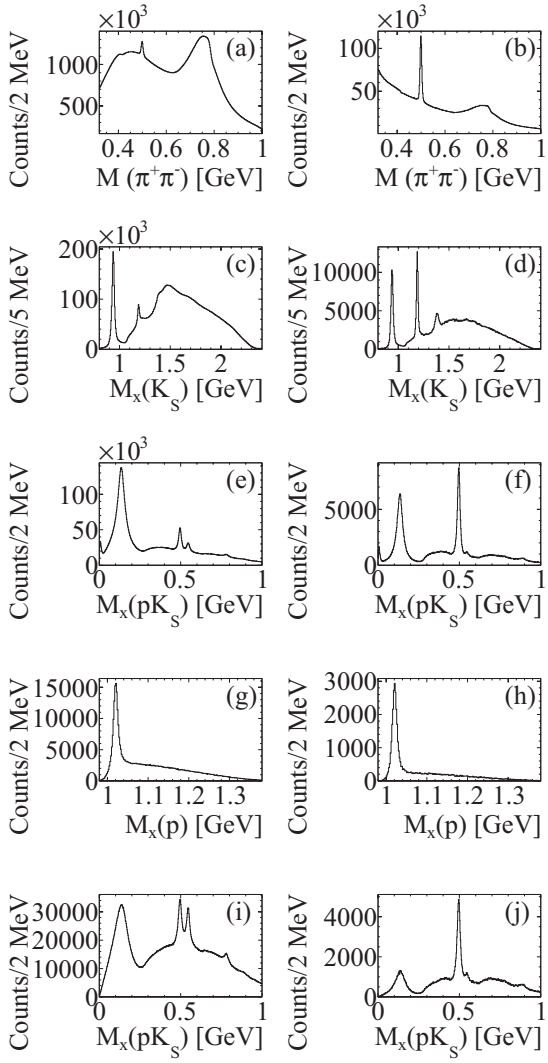

FIG. 2. Upper row: invariant mass of oppositely charged pions; second row: missing mass of K_S; third row: missing mass of pK_S system; fourth row: missing mass of the proton with the cuts $M(\pi^+\pi^-) = 0.497 \pm 0.01$ GeV and $M_X(pK_S) = 0.497 \pm 0.02$ GeV; fifth row: missing mass of pK_S system for events above $M_X(p) > 1.04$ GeV. All figures in the left column are without the vertex cuts and all figures in the right column are with the vertex cuts.

the proton track and the photon beam line is called the primary vertex.

(ii) The distance of closest approach of the two pion tracks must be less than 1.5 cm; the midpoint of the shortest line between the two pion tracks is called the decay vertex.

(iii) $\cos\theta_c > 0.96$; the collinearity angle, θ_c, is the angle between the line connecting the primary and decay vertices and the direction of the three-momentum of the K_S reconstructed as the sum of the two pion momenta.

The impact of the vertex and particle identification cuts are presented in Fig. 2. In this figure, all mass distributions in the left column are without the vertex cuts described above, and those in the right column are with the vertex cuts.

(i) The upper row shows the invariant mass of the two pions with K_S at ~ 0.5 GeV. The collinearity cut preferentially selects events with a separated $K_S \to \pi^+\pi^-$ decay vertex. This reduces the K_S signal by roughly a factor of $\sim$2, but it reduces the nonstrange $\pi^+\pi^-$ continuum by a factor of $\sim$30. Thus the ρ peak at 0.76 GeV is prominent in the left plot and the K_S peak at 0.5 GeV is prominent in the right-hand plot.

(ii) In the second row, the missing mass of K_S, $M_X(K_S)$, $M_X(K_S)^2 = (P_\gamma + P_p - P_{K_S})^2$, where $P_i (i = \gamma, p, K_S)$ is the four-momentum of a given particle, is plotted by selecting events within $M_{\pi^+\pi^-} = 0.497 \pm 0.010$ GeV. In the right panel, Fig. 2(d), one sees prominent peaks for the proton, $\Sigma(1189)^+$ and $\Sigma(1385)^+$ states, while on the left panel [Fig. 2(c), without the vertex cuts] the $\Sigma(1385)^+$ state is hardly visible. Moreover, the vertex cuts substantially enhance the $\Sigma(1189)^+$ signal relative to the proton peak in Fig. 2(d) compared to Fig. 2(c). This is a consequence of the fact that the vertex cuts, particularly the collinearity cut, strongly reduce the nonresonant $\pi\pi$ continuum, which is not associated with strangeness production.

(iii) In the third row we show the missing mass of the proton and K_S, $M_X(pK_S)$, $M_X(pK_S)^2 = (P_\gamma + P_p - P_{K_S} - P_{p'})^2$, where $P_{p'}$ is a four-momentum of the final-state proton, showing the π^0, K^0, and η peaks in Fig. 2(e). As one can see in Fig. 2(f), with the vertex cuts the signal-to-background ratio of the missing kaon is significantly improved, the η peak almost vanishes, and the π^0 peak, as a decay product of $\Sigma(1189)^+ \to p\pi^0$, is still prominent.

(iv) The fourth row shows the missing mass of the proton, $M_X(p)$, $M_X(p)^2 = (P_\gamma + P_p - P_{p'})^2$, by selecting K_S ($M_{\pi^+\pi^-} = 0.497 \pm 0.010$ GeV) and K_L [$M_X(pK_S) = 0.497 \pm 0.020$ GeV] from the first and third rows. One can see a peak for the ϕ meson in both cases: without [Fig. 2(g)] and with [Fig. 2(h)] vertex cuts. Again the signal-to-background ratio is significantly improved with the vertex cuts.

(v) Finally, in the fifth row [Figs. 2(i) and 2(j)] we show again the missing mass of the proton and K_S, $M_X(pK_S)$, this time plotted only for events outside the ϕ peak, i.e., $M_X(p) > 1.04$. The left panel corresponds to the event selection used in the previous CLAS analysis of these data [16].

From Fig. 2 one can conclude that the application of the vertex cuts significantly improves the identification of the final-state particles.

In Fig. 3 the missing mass of K_S is presented without vertex cuts and for events above the ϕ peak, $M_\phi > 1.04$ GeV. The upper panel [Fig. 3(a)] is for events without a cut on the K_L peak. Although there are many events in the distribution, a prominent state such as the $\Sigma(1385)^+$ is barely visible on top of a very high background. By applying an additional cut on the K_L peak we reproduce the CLAS published analysis [16]

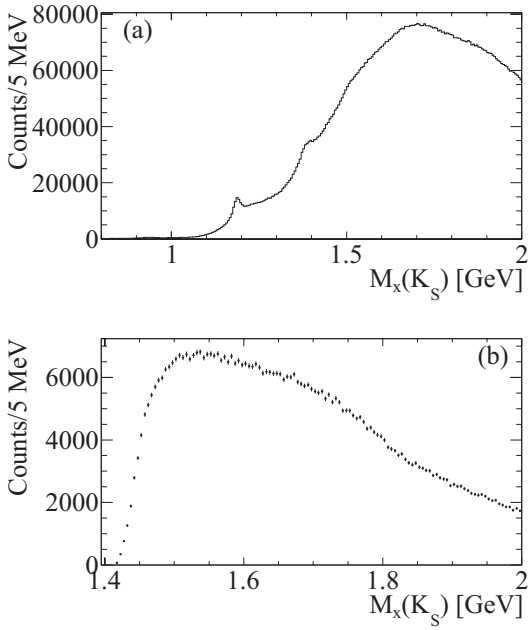

FIG. 3. Upper panel: missing mass of K_S without vertex cuts and no cut on the K_L peak. Lower panel: missing mass of K_S without vertex cuts, but with the cut on the K_L peak. Both histograms are for events selected above the ϕ peak $M_\phi > 1.04$ GeV.

and obtain a similar structureless distribution, as presented in Fig. 3(b). The upper limit of the Θ^+ photoproduction cross section in [16] was estimated from this distribution.

B. Interference with ϕ production

In this section we present our results for pK_LK_S events selected under the ϕ peak. The main goal is to study the missing mass of K_S, which is equivalent to the invariant mass of the final-state proton and missing K_L, $M_X(K_S) = M(pK_L)$. This kinematic domain has not been studied before and, as discussed in the introduction, might possibly reveal a tiny signal in the missing mass of K_S due to interference with the very strong signal of ϕ production.

In Fig. 4 the incoming photon beam energy is plotted versus $M_X(K_S)$ for events selected under the ϕ peak with a cut

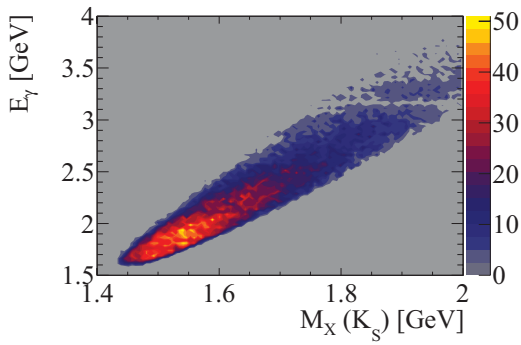

FIG. 4. (Color online) Incoming photon beam energy vs $M_X(K_S)$ for events selected under the ϕ peak.

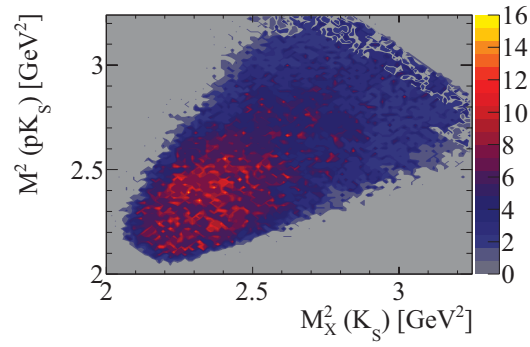

FIG. 5. (Color online) Dalitz plot showing invariant mass $M^2(pK_S)$ vs $M^2_X(K_S)$ for events selected under the ϕ peak.

$M_X(p) = 1.02 \pm 0.01$ GeV. Photons above 2.4 GeV do not contribute to the region of $M_X(K_S) = (1.5\text{–}1.6)$ GeV, where previously signals for a resonance in the KN system have been reported. Therefore in the following we used data with a safe upper limit cut of $E_\gamma < 2.6$ GeV, which at the same time includes a sufficiently wide range of photon energy to control the phase-space distribution of ϕ production.

In order to see the whole kinematic phase space, in Fig. 5 we present the Dalitz plot, $M(pK_S)^2$ versus $M(pK_L)^2$, for events selected under the ϕ peak, $M_X(p) = 1.02 \pm 0.01$ GeV. To perform a search for a resonance structure in the missing mass of K_S, i.e., $M(pK_L)$, we need to restrict kinematic overlap with another system created in the invariant mass $M(pK_S)$, such as the well-known Σ^* resonances, which could affect and wash out a possible signal for a narrow structure.

In Fig. 6 $M_X(K_S)$ is presented with different cuts on the invariant mass $M(pK_S)$, namely no cut (vertex cuts only) [Fig. 6(a)] with total number of events $N_{\text{events}} = 20\,007$, with the cut $M(pK_S) < 1.56$ GeV [Fig. 6(b)] with $N_{\text{events}} = 6766$, with the cut $M(pK_S) < 1.52$ GeV [Fig. 6(c)] with $N_{\text{events}} = 3744$, and with the cut $M(pK_S) < 1.5$ GeV [Fig. 6(d)] with $N_{\text{events}} = 2380$. As one can see, there are hints of some structure around 1.54 GeV. By gradually changing the cut on $M(pK_S)$ the peak structure in $M_X(K_S)$ becomes more and more prominent.

Next in Fig. 7 we plot the Chew-Low diagram, t_Θ versus $M_X(K_S)$. Here t_Θ is defined as $t_\Theta = (P_\gamma - P_{K_S})^2$, where P_γ and P_{K_S} are four-momenta of the incoming photon and reconstructed K_S. Since we do not know the mechanism for photoproduction of the possible resonance in the $M(pK_L)$ system, we assumed that it should be produced with some exponential t dependence, like other baryons, such as $\Lambda(1520)$. Therefore we expected that by selecting lower t_Θ values we would suppress the background without losing too many signal events. In Fig. 8 the distribution of $M_X(K_S)$ is presented without a cut on t_Θ [Fig. 8(a)] with $N_{\text{events}} = 20\,007$, with a cut $-t_\Theta < 0.55$ GeV^2 [Fig. 8(b)] with $N_{\text{events}} = 10\,590$, with a cut $-t_\Theta < 0.45$ GeV^2 [Fig. 8(c)] with $N_{\text{events}} = 5271$, and with a cut $-t_\Theta < 0.4$ GeV^2 [Fig. 8(d)] with $N_{\text{events}} = 2848$. Figure 8 does not include a $M(pK_S)$ cut. The statistical significance of the structure at $\sim$1.54 GeV is maximized for values of $-t_\Theta < 0.45$ GeV^2. By applying a tighter cut, $-t_\Theta < 0.4$ GeV^2 [Fig. 8(d)], we lose statistics and the statistical significance

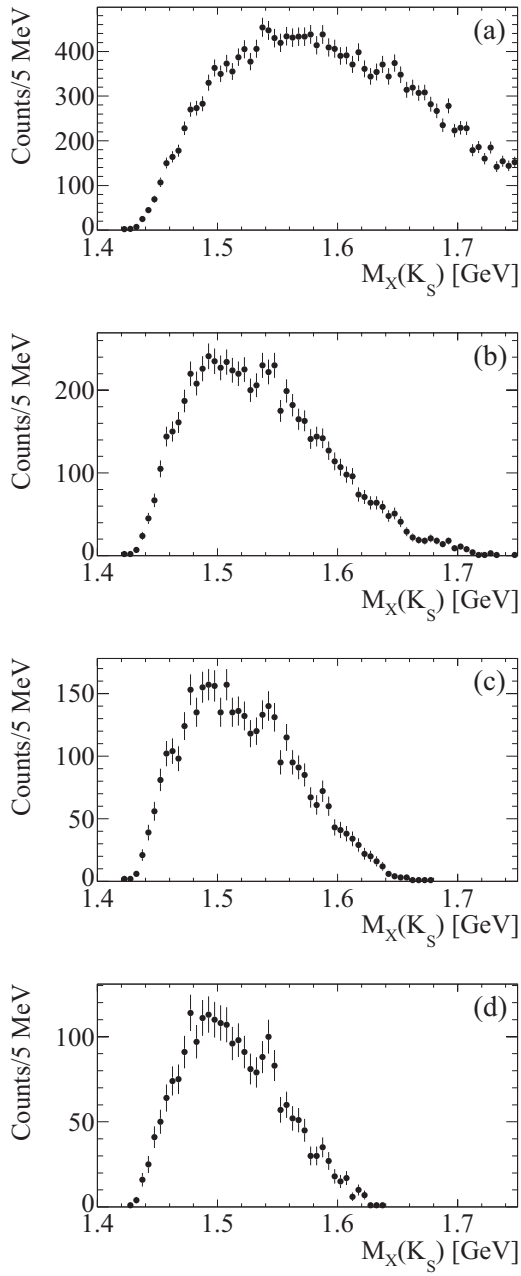

FIG. 6. Missing mass of K_S plotted with different cuts on the invariant mass $M(pK_S)$: (a) no cuts (vertex cuts only), (b) $M(pK_S) <$ 1.56 GeV, (c) $M(pK_S) < 1.52$ GeV, and (d) $M(pK_S) < 1.5$ GeV.

of the observed structure deteriorates. We note that the significance of the structure at 1.54 GeV does not vary as one would expect purely from the statistics. This could be the result of a complicated interference between the ϕ and the baryon resonance. For example, the ϕ production mechanism changes at about $t_\phi = (P_\gamma - P_\phi)^2 \approx -0.5$ GeV^2 from predominantly diffractive (at lower $|t_\phi|$) to predominantly s channel [27,28]. If the phase of the interference depends on the ϕ production mechanism, then integrating over different mechanisms could wash out a possible signal in the pK_L system. Moreover, s-channel ϕ production decreases much more slowly with t_ϕ than diffractive ϕ production. Thus, inclusion of the s-channel

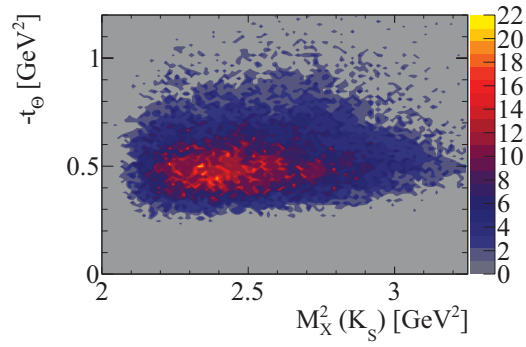

FIG. 7. (Color online) Chew-Low diagram showing t_Θ vs $M_X^2(K_S)$ for events selected under the ϕ peak.

mechanism could further decrease the signal-to-background ratio. The cut on t_Θ also significantly reduces the range of t_ϕ, thereby reducing the s-channel contribution and potentially improving the signal-to-background ratio.

From Figs. 6 and 8 one can see that the resonance structure around 1.54 GeV appears either by restricting the $M(pK_S)$ invariant mass or by selecting the low-t_Θ region.

We are unable to find any significant peak in the invariant mass spectrum $M(pK_S)$. This is because the resolution of low-momentum protons is significantly worse in CLAS than the photon energy resolution. The $p\,K_L$ mass is computed from the missing mass $M_X(\gamma p \to \pi^+\pi^- X)$ and depends only on the pion and photon resolutions. The $p\,K_S$ mass is computed from the $p\,\pi^+\pi^-$ mass and depends on both the pion and proton resolutions. Detailed Monte Carlo studies have shown that the CLAS resolution for the invariant mass $M(p\,K_S)$ is much worse than for the missing mass $M_X(\gamma p \to \pi^+\pi^- X)$ due to the use of low-momenta protons in the reconstruction of the invariant mass. Similarly, a generated narrow peak is not reconstructed as part of the Monte Carlo simulation of the $M(pK_S)$ spectrum, whereas the same peak generated in the $M_X(K_S)$ spectrum can be clearly reconstructed.

In Fig. 9 we plot $-t_\Theta$ versus $M(pK_S)^2$ to see whether there is any correlation between these two variables due to the limited CLAS acceptance, although these two variables are in general independent. As one can see, there is no strong correlation, just as expected.

IV. MONTE CARLO SIMULATION AND STATISTICAL SIGNIFICANCE OF THE OBSERVED STRUCTURE

In our analysis we looked for a possible resonance structure that interferes with ϕ production in the final state $K_S K_L p$. We looked for deviation of the missing mass spectra of K_S in the experimental data from the missing mass of K_S for pure ϕ production.

Our ϕ photoproduction Monte Carlo simulation is based on the Titov-Lee model [28]. The angular dependencies of ϕ decay were taken from the pomeron exchange model and the energy dependence of ϕ production was modeled using several iterations in the simulation. The t dependence of ϕ production was simulated with an exponential function $\exp(b_\phi t_\phi)$, where $t_\phi = (P_\gamma - P_\phi)^2$, with the slope $b_\phi = 3.4$ GeV^{-2} taken from

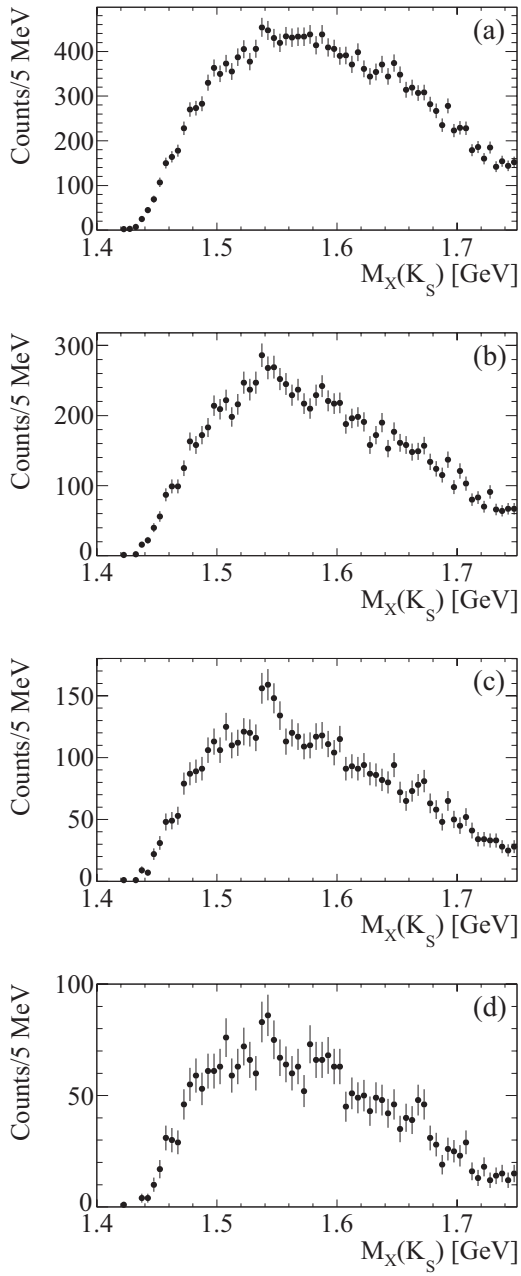

FIG. 8. Missing mass of K_S with different cuts on t_Θ: (a) with no cut on t_Θ, (b) $-t_\Theta < 0.55$ GeV^2, (c) $-t_\Theta < 0.45$ GeV^2, and (d) $-t_\Theta < 0.4$ GeV^2.

the existing data [29]. The model describes experimental data quite well in the low-t_ϕ region, where ϕ production due to the pomeron exchange mechanism dominates.

Simulated events were passed through the CLAS detector emulation program (GSIM) and then were reconstructed with RECSIS (the CLAS reconstruction program). The Monte Carlo simulated data were analyzed using the same programs and the obtained distributions (with the same cuts as for the data) were compared to the missing mass of K_S from experimental data.

In Fig. 10 the experimental distribution of the missing mass of K_S, $M_X(K_S)$, is presented with the cut on $-t_\Theta < 0.45$ GeV^2.

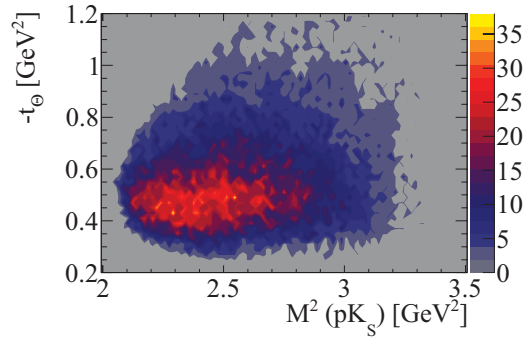

FIG. 9. (Color online) Plot of $-t_\Theta$ vs $M(pK_S)^2$ for events selected under the ϕ peak, $M_X(p) = 1.02 \pm 0.01$ GeV.

The dashed line is the result of the Monte Carlo simulation, which is a smooth distribution without any structure. To account for imperfections in the detector simulation, we allowed this distribution to vary slightly to describe the data better.

For this, the missing mass distribution is fitted using the function

$$F_B = SIM(\phi) \cdot POL_3, \tag{1}$$

where $SIM(\phi)$ is the Monte Carlo simulated histogram from ϕ production, and POL_3 is a third-order polynomial function. All parameters of the POL_3 function were allowed to vary. The result is the dashed-dotted line in Fig. 10; we refer to that distribution (F_B) as the null or background (B) hypothesis, i.e., assuming that the experimental spectrum is fully described by the modified Monte Carlo distribution.

A second hypothesis assumes that, in addition to the background described by the null hypothesis, there is a resonance structure, which is chosen to have Gaussian (G) shape.

This is called the signal + background hypothesis (S + B) and is fit with the following function:

$$F_{S+B} = SIM(\phi) \cdot POL_3 + G, \tag{2}$$

shown as the solid line in Fig. 10.

To estimate the statistical significance of the observed resonance structure we performed a log-likelihood test of the

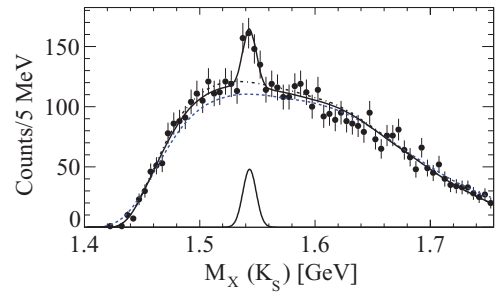

FIG. 10. (Color online) Missing mass of K_S with a cut $-t_\Theta < 0.45$ GeV^2. The dashed line is the result of a ϕ Monte Carlo simulation, the dashed-dotted line is a modified Monte Carlo distribution, and the solid line is the result of a fit with a modified Monte Carlo distribution plus a Gaussian function.

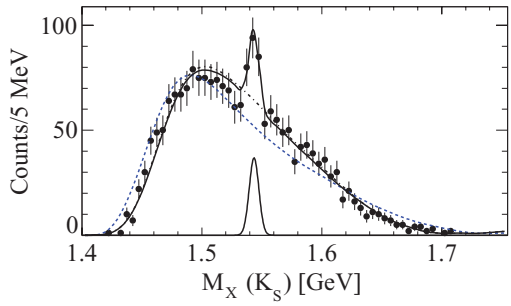

FIG. 11. (Color online) Missing mass of K_S with cuts $-t_\Theta < 0.45$ GeV^2 and $M(pK_S) < 1.56$ GeV. The dashed line is the result of a ϕ Monte Carlo simulation, the dashed-dotted line is a modified Monte Carlo distribution, and the solid line is the result of a fit with a modified Monte Carlo distribution plus a Gaussian function.

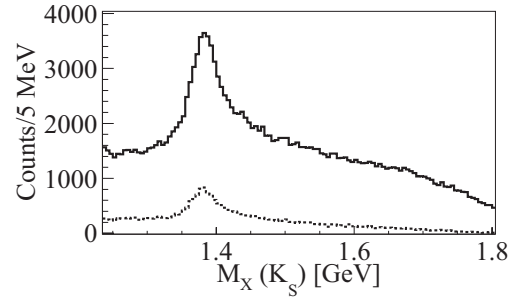

FIG. 12. Missing mass of K_S for events with $|M_X(pK_S) - 0.497| > 0.03$ GeV. The solid histogram is for events without any cut on t_Σ, and the dashed histogram is for those with a cut $-t_\Sigma < 0.45$ GeV^2.

two hypotheses:

$$-2\ln\mathcal{L}_{S+B} = 2\sum_{i=0}^{N}[(s_i+b_i) - n_i + n_i\ln(n_i/(s_i+b_i))] \tag{3}$$

$$-2\ln\mathcal{L}_{B} = \sum_{i=0}^{N}[b_i - n_i + n_i\ln(n_i/b_i)], \tag{4}$$

where $\mathcal{L}_{S+B}$ and $\mathcal{L}_B$ are likelihoods for S + B and B hypotheses respectively, n_i is the total number of events in the ith bin, and b_i and s_i are the numbers of predicted background and signal events, respectively, in the given bin. The peak parameters obtained from the fit are $M_X(K_S) = 1.543 \pm 0.002$ GeV with a Gaussian width $\sigma = 0.006 \pm 0.001$ GeV, compatible with the experimental resolution of CLAS [16].

To demonstrate how well the Monte Carlo simulation reproduces the shape of the experimental distribution and to see the robustness of the significance of the observed signal, we present the $M_X(K_S)$ distribution with cuts on $-t_\Theta < 0.45$ GeV^2 and invariant mass $M(pK_S) < 1.56$ GeV in Fig. 11. The additional cut on the invariant mass $M(pK_S)$ changes the shape of the experimental distribution significantly. Now the resonance structure appears on top of a background with inclined shape and not in the middle of the symmetric distribution, as in Fig. 10. The fit values for the peak are $M_X(K_S) = 1.543 \pm 0.001$ GeV with a Gaussian width $\sigma = 0.004 \pm 0.001$ GeV.

In Table I we summarize statistical information about hypotheses testing based on data presented in Figs. 10 and 11 as a result of the fits described above. For each of these figures there are two rows with the fit corresponding to S + B and B hypotheses. The columns represent number of degrees of freedom (ndf), χ^2, p value, and log likelihood, ln $\mathcal{L}$, for a given hypothesis. The seventh column is twice the log-likelihood ratio of two hypotheses, $2\Delta(\ln\mathcal{L})$, a square root of which for one-degree-of-freedom difference between the two hypotheses would have normally represented statistical significance in number of σ's; however, in our case with $\Delta\text{ndf} = 3$, it will be lower. To avoid obtaining artificially high statistical significance we took into account the fact that the hypothesis with the fewer degrees of freedom has an advantage to fit data better. To do this we recalculated $\sqrt{2\Delta(\ln\mathcal{L})} = \sqrt{\chi^2_{(\Delta\text{ndf}=1)}}$ significance for one-degree-of-freedom difference using a p value corresponding to $\chi^2_{(\Delta\text{ndf}=3)} = 2\Delta(\ln\mathcal{L})$ for three degrees of freedom. The obtained significance (5.3σ for Fig. 10 and 4σ for Fig. 11) is presented in the column labeled S, in units of σ. The fitted signal yield (number of events), i.e., the integral of the Gaussian distribution, is presented in the last column with statistical errors from the fit.

As strangeness in the pK_L system is not fixed, the structure in Figs. 10 and 11 may be due to an unobserved Σ^{*+} resonance, which decays into $p\bar{K}^0$. However, Σ^{*+} should also decay to $\Lambda\pi$, $\Lambda\pi\pi$, $\Sigma\pi$, $\Sigma\pi\pi$, etc. In order to check this possibility, in Fig. 12 we plot the missing mass of K_S, $M_X(K_S)$, for events outside the peak of the missing kaon, $|M_X(pK_S) - 0.497| > 0.03$ GeV. As one can see, there is a clear peak of $\Sigma(1385)$, but no narrow resonance structure is seen at ~1.54 GeV either without a cut on $t_\Sigma = (P_\gamma - P_{K_S})^2$ (solid histogram) or with a cut $-t_\Sigma < 0.45$ GeV^2 (dashed histogram). Figure 12 demonstrates also that the set of cuts which we use in our analysis (vertex cuts and t_Θ cut) does not produce by itself any artificial peaks.

TABLE I. Fit results (see text for explanation).

Figure	Fit	ndf	χ^2	p	$-2\ln\mathcal{L}$	$2\Delta(\ln\mathcal{L})$	S	Signal yield
Fig. 10	S + B	67	52	0.91	54	31	5.3σ	142 ± 46
	B	70	79	0.22	85			
Fig. 11	S + B	46	37	0.82	40	22	4σ	83 ± 27
	B	49	55	0.24	62			

V. CONCLUSIONS

To conclude, we use, for the first time, meson-baryon interference to search for a weak baryon resonance in the same final state. This search was motivated by a desire to increase the sensitivity of the CLAS detector to a possible pentaquark state. We observe a narrow structure in the data at $M_X(K_S) = 1.543$ GeV with a Gaussian width $\sigma = 0.006$ GeV for the reaction $\gamma p \to p K_S K_L$ when $M(K_S K_L) = m_\phi$ and $-t_\Theta < 0.45$ GeV^2. Because we are looking for a peak in the interference between a resonance in the KN system and ϕ production, all of our background is due to ϕ production. This puts us in the advantageous position of understanding the background in our reaction. The peak is not reproduced by the Monte Carlo simulation that accurately describes the essential background of ϕ production.

The statistical significance of the observed signal, estimated as a log-likelihood ratio of signal + background and background-only hypotheses, is 5.3σ. When we vary the background by cutting on the invariant mass $M(pK_S)$, the peak remains significant.

The best explanation for the observed structure is interference between ϕ and KN resonance production. Since strangeness is not fixed in this reaction, there are two possibilities for the origin of the observed structure. It may be due to the photoproduction of the Θ^+ pentaquark or some unknown Σ^* resonance. As we did not observe a narrow Σ^{*+} decaying to ground-state Λ and Σ hyperons, it is unlikely for the observed structure to be due to a Σ^* resonance. Note that the interference can shift the peak position from the actual resonance position. To simulate in detail the interference between two subprocesses one needs to have much more information, including the cross section and width of the baryon resonance, the slope of its t dependence, and the relative phase of the interfering amplitudes. The existing data set is too small to constrain reliably any of these parameters, so we leave such studies for the future.

The present result does not contradict the previous CLAS analysis in the same channel [16] that did not observe a peak near 1.54 GeV, since events with $M(K_S K_L) = m_\phi$ were excluded there with the cut $m_X(p) > 1.04$ GeV. Assuming that the observed peak is mainly due to ϕ-KN interference, we estimated the photoproduction cross section of the KN resonance with a Breit-Wigner width $\Gamma = 1$ MeV to be two orders of magnitude smaller than the photoproduction cross section of the ϕ meson, consistent with the few-nanobarn upper limit of the cross section established by the CLAS Collaboration [16] for the photoproduction of Θ^+.

In addition, because the peak in these data is only observed at relatively small values of t_θ, this might reconcile the CLAS null results [16] and the SPring-8 observation of the Θ^+ [21] in similar channels. The CLAS acceptance at $-t_\Theta < 0.5$ GeV^2 is much smaller than that of SPring-8.

Nevertheless, we are not without unanswered questions. One of those questions is the following: If the observed signal is due to the interference with ϕ-meson production, why does the statistical significance of the signal sharply diminish at higher values of t_Θ? Is it because the phase of the interference has a strong t dependence or is it because the mechanism of ϕ production changes from pomeron exchange to the excitation of intermediate baryon resonances and therefore an increase of statistics in ϕ production does not necessarily guarantee the same increase in the interference term?

Another question relates to why restrictions on the invariant mass of the pK_S system effectively enable this signal to manifest itself, even without the t cut. Is it possible that well-known excited Σ^* resonances listed in [17] interfere destructively with the ϕ and affect the narrow structure we observe at 1.54 GeV?

To answer these questions, to further corroborate the existence of a resonance underlying the observed structure, to elucidate its quantum numbers, and to understand the details of the interference, additional data for this and other channels are needed.

The interpretation of experimental results obtained in this analysis reflects the opinion of the authors and not that of the CLAS Collaboration as a whole.

ACKNOWLEDGMENTS

We would like to acknowledge the outstanding efforts of the staff members of the Accelerator and the Physics Divisions at Jefferson Lab who made the experiment possible. This work was supported in part by the Italian Istituto Nazionale di Fisica Nucleare, the French Centre National de la Recherche Scientifique and Commissariat à l'Energie Atomique, the US Department of Energy and National Science Foundation, and the Korea Science and Engineering Foundation. The Southeastern Universities Research Association (SURA) operates the Thomas Jefferson National Accelerator Facility for the United States Department of Energy under Contract No. DEAC05-84ER40150. The work of M.V.P. is supported by the DFG SFB/TR16 Program (Germany). Ya.A. is partly supported by the Russian State Grant No. RSGSS-65751.2010.2.

[1] D. Diakonov, V. Petrov, and M. V. Polyakov, Z. Phys. A **359**, 305 (1997).
[2] T. Nakano *et al.*, Phys. Rev. Lett. **91**, 012002 (2003).
[3] V. V. Barmin *et al.* (DIANA Collaboration), Phys. At. Nucl. **66**, 1715 (2003); V. V. Barmin *et al.* (DIANA Collaboration), Yad. Fiz. **66**, 1763 (2003).
[4] S. Stepanyan *et al.* (CLAS Collaboration), Phys. Rev. Lett. **91**, 252001 (2003).
[5] V. Kubarovsky *et al.* (CLAS Collaboration), Phys. Rev. Lett. **92**, 032001 (2004).
[6] J. Barth *et al.* (SAPHIR Collaboration), Phys. Lett. B **572**, 127 (2003).
[7] A. Airapetian *et al.* (HERMES Collaboration), Phys. Lett. B **585**, 213 (2004).
[8] S. Chekanov *et al.* (ZEUS Collaboration), Phys. Lett. B **591**, 7 (2004).
[9] A. Aleev *et al.* (SVD Collaboration), Yad. Fiz. **68**, 1012 (2005).
[10] I. Abt *et al.* (HERA-B Collaboration), Phys. Rev. Lett. **93**, 212003 (2004).

[11] M. J. Longo *et al*. (HyperCP Collaboration), Phys. Rev. D **70**, 111101 (2004).
[12] J. Z. Bai *et al*. (BES Collaboration), Phys. Rev. D **70**, 012004 (2004).
[13] R. Barate *et al*. (ALEPH Collaboration), Phys. Lett. **599**, 1 (2004).
[14] B. Aubert *et al*. (BABAR Collaboration), Phys. Rev. Lett. **95**, 042002 (2005).
[15] B. McKinnon *et al*. (CLAS Collaboration), Phys. Rev. Lett. **96**, 212001 (2006).
[16] R. De Vita *et al*. (CLAS Collaboration), Phys. Rev. D **74**, 032001 (2006)
[17] K. Nakamura *et al*. (Particle Data Group), J. Phys. G **37**, 075021 (2010).
[18] K. Hicks, Progr. Part. Nucl. Phys. **55**, 647 (2005).
[19] V. D. Burkert, Int. J. Mod. Phys. A **21**, 1764 (2006).
[20] Y. Azimov, K. Goeke, and I. Strakovsky, Phys. Rev. D **76**, 074013 (2007).
[21] T. Nakano *et al*., Phys. Rev. C **79**, 025210 (2009).
[22] V. V. Barmin *et al*. (DIANA Collaboration), Phys. Atom. Nucl. **70**, 35 (2007).
[23] V. V. Barmin *et al*. (DIANA Collaboration), Phys. Atom. Nucl. **73**, 1168 (2010).
[24] Ya. Azimov, J. Phys. G: Nucl. Part. Phys. **37**, 023001 (2010).
[25] M. Amarian, D. Diakonov, and M. V. Polyakov, Phys. Rev. D **78**, 074003 (2008).
[26] B. Mecking *et al*., Nucl. Instrum. Methods A **503**, 513 (2003).
[27] R. A. Williams, Phys. Rev. C **57**, 223 (1998).
[28] A. I. Titov and T. S. H. Lee, Phys. Rev. C **67**, 065205 (2003).
[29] T. Mibe *et al*. (LEPS Collaboration), Phys. Rev. Lett. **95**, 182001 (2005).